HSATII RNA is induced via a noncanonical ATM-regulated DNA damage response pathway and promotes tumor cell proliferation and movement

Maciej T. Nogalski[a,1] and Thomas Shenk[a,1]

[a]Department of Molecular Biology, Princeton University, Princeton, NJ 08544-1014

Contributed by Thomas Shenk, October 21, 2020 (sent for review August 21, 2020; reviewed by Charles S. Cobbs and Timothy F. Kowalik)

Pericentromeric human satellite II (HSATII) repeats are normally silent but can be actively transcribed in tumor cells, where increased HSATII copy number is associated with a poor prognosis in colon cancer, and in human cytomegalovirus (HCMV)-infected fibroblasts, where the RNA facilitates viral replication. Here, we report that HCMV infection or treatment of ARPE-19 diploid epithelial cells with DNA-damaging agents, etoposide or zeocin, induces HSATII RNA expression, and a kinase-independent function of ATM is required for the induction. Additionally, various breast cancer cell lines growing in adherent, two-dimensional cell culture express HSATII RNA at different levels, and levels are markedly increased when cells are infected with HCMV or treated with zeocin. High levels of HSATII RNA expression correlate with enhanced migration of breast cancer cells, and knockdown of HSATII RNA reduces cell migration and the rate of cell proliferation. Our investigation links high expression of HSATII RNA to the DNA damage response, centered on a noncanonical function of ATM, and demonstrates a role for the satellite RNA in tumor cell proliferation and movement.

HSATII | human satellite II | DNA damage response | human cytomegalovirus | breast cancer cells

Repetitive DNA sequences comprise more than 50% of the human genome (1) and include short (SINE) and long (LINE) interspersed nuclear elements, DNA transposons, long terminal repeat transposons, and satellite repeats. Even though repetitive DNA elements are ubiquitous in the human genome, there is a relatively limited understanding of their functions and the molecular mechanisms regulating their expression. Satellite DNAs (satDNAs), which account for ∼3% of the genome (1), are constituents of centromeric and pericentromeric heterochromatin, and have been implicated in chromosome organization and segregation, kinetochore formation, as well as heterochromatin regulation (2). Next-generation sequencing showed these genomic sites, originally thought to be largely transcriptionally inert, can produce noncoding RNAs (ncRNAs), contributing to satDNA functions (3–6).

Altered patterns of transcription, including the induction of ncRNA accumulation, occur in tumors (7–9). Several ncRNAs originating from satDNA regions of the genome are expressed in cancer cells, such as human alpha-satellite repeat (Alpha/ALR) RNA, human satellite II (HSATII) RNA, and its mouse counterpart GSAT RNA (10–15). While some satDNA transcription is stress dependent (16) or triggered during apoptotic, differentiation, or senescence programs in cells (17, 18), HSATII RNA accumulation was found to be refractory to these generalized stressors. Rather, it was induced in a series of colorectal cancer cells when they were grown under nonadherent conditions or as xenografts in mice (19). High expression of Alpha/ALR and HSATII RNAs can lead to their reverse transcription and stable reintegration into the human genome, expanding their genomic copy numbers (19). Elevated copies of genomic HSATII sequences were found in primary human colon tumors and correlated with lower survival rates of colon cancer patients (19). Ectopically expressed Alpha/ALR RNA was found to induce tumor formation in mice (15). Additionally, HSATII and GSAT RNAs have a nucleotide motif usage that is distinct from that commonly seen in most noncoding transcripts, resulting in their immunostimulatory potential (20).

Viruses deregulate many biological processes, often in a similar manner to aberrations seen in cancer cells. Those biological changes caused by infections not only resemble cancer, but in some cases contribute to oncogenesis (21). Indeed, it is estimated that 12 to 20% of all cancers have a viral etiology and often are linked to persistent or chronic viral infections (22–24).

Human cytomegalovirus (HCMV) is a β-herpesvirus that infects a large percentage of the adult population worldwide. Infection in immunocompetent people is typically asymptomatic. In contrast, HCMV is a life-threatening opportunistic pathogen in immunosuppressed individuals (25–27), and a major infectious cause of birth defects (28). Many of the biological changes seen in HCMV-infected cells resemble those common to cancers, including activation of pro-oncogenic pathways, changes in cellular metabolism, and increased cell survival (29–34). Given similarities in the molecular symptoms of HCMV infections and tumorigenesis, as well as its reliable presence in glioblastoma tumors, HCMV has been suggested to play a role, perhaps an oncomodulatory role, in the etiology of several human cancers

Significance

HSATII RNA is associated with cancer progression and immunostimulation, and as we recently reported, it plays an important role in herpesvirus infections. However, our understanding of cellular processes responsible for the expression of HSATII RNA is limited. Our current investigation identified a noncanonical, ATM kinase-independent DNA damage response pathway as a common cellular mechanism regulating HSATII RNA induction in virus-infected cells or cells treated with DNA-damaging agents. Additionally, our study provides a link between expression of HSATII RNA and the cellular growth and migration phenotypes of cancer cells, establishing a paradigm to study the biological consequences of HSATII RNA expression, i.e., treatment of normal diploid and tumor cells with DNA-damaging agents.

Author contributions: M.T.N. and T.S. designed research; M.T.N. performed research; M.T.N. and T.S. analyzed data; and M.T.N. and T.S. wrote the paper.

Reviewers: C.S.C., Swedish Neuroscience Institute Seattle; and T.F.K., University of Massachusetts Medical School.

Competing interest statement: Icahn School of Medicine at Mt. Sinai and Princeton University have submitted a provisional patent application based on the use of HSATII-specific LNAs for HSATII knockdown, and M.T.N. and T.S. are co-inventors.

[1]To whom correspondence may be addressed. Email: nogalski@princeton.edu or tshenk@princeton.edu.

This article contains supporting information online at https://www.pnas.org/lookup/suppl/doi:10.1073/pnas.2017734117/-/DCSupplemental.

(31, 35–41). However, its high prevalence has made it difficult to establish causality in the disease (42).

Recently, we determined that HCMV infection induces HSATII RNA in fibroblasts, among other satDNA transcripts, to a similar extent as reported for tumor cells (43). Elevated HSATII RNA was also detected in biopsies of CMV colitis, showing that the RNA is elevated in human infections and raising the possibility that elevated HSATII RNA may influence the pathogenesis of HCMV disease. When the amount of HSATII RNA in HCMV-infected fibroblasts was reduced by knockdown (KD) with locked nucleic acid (LNA) oligonucleotides, viral gene expression, DNA accumulation, and yield were reduced. Moreover, KD experiments revealed that HSATII RNA affects several infected-cell processes, including protein stability, posttranslational modifications, and motility of infected cells.

The HCMV IE1 and IE2 proteins induce HSATII RNA (43) and are known to regulate the Rb and E2F protein families, which contribute to efficient viral replication in part through induction of a DNA damage response (DDR) (44, 45). Here, we have tested the possibility that these two activities of the viral IE1 and IE2 proteins—induction of a DDR and HSATII RNA—are related. We report that the DNA-damaging agents, zeocin and etoposide, which induce DNA double-strand breaks (DSBs) and a DDR (46, 47), markedly induce HSATII RNA in diploid epithelial cells growing in adherent, two-dimensional culture. Consistent with this observation, ATM, a key regulator of DDRs, is required for induction of the satellite RNA by infection or DNA-damaging agents. Importantly, HSATII RNA induction requires a noncanonical, kinase-independent ATM function. Finally, we demonstrate that HSATII RNA is expressed in a variety of breast cancer cell lines grown in adherent culture, the RNA is further induced in these cell lines by HCMV infection or zeocin treatment, and HSATII RNA levels correlate with their migration and proliferation rates. In sum, our data argue that the DDR leads to elevated HSATII RNA levels, potentially enhancing the fitness of both HCMV and tumor cells.

Results

The DDR Regulates HSATII RNA Expression. Ectopic expression of the HCMV IE1 and IE2 proteins can induce HSATII RNA expression in the absence of infection (43). As IE1 and IE2 induce a DDR that supports efficient viral replication (44, 45), we speculated that the DDR could play a role in the expression of human satDNAs.

To test this hypothesis, ARPE-19 cells were stressed by three regimens that induce a DDR: UV-C irradiation, H_2O_2 treatment, or serum withdrawal (48–50). Exposure of these diploid epithelial cells, which normally express HSATII RNAs at very low basal levels, to stressing agents induced HSATII RNA to a very limited extent, 2- to 3-fold (Fig. 1*A*), in contrast to the 100- to 1,000-fold induction observed in response to virus infection (43). As a proxy to monitor successful DDR activation, the induction of p53 activity was monitored by assaying the levels of p53-dependent cyclin-dependent kinase inhibitor 1 (p21; encoded by the CDKN1A gene) (48) and p53-regulated damage-induced noncoding (DINO) long noncoding RNA (lncRNA) (51). As expected, both were elevated in cells exposed to all three treatments (Fig. 1*A*).

We reasoned that the failure of these treatments to induce HSATII RNA might be a consequence of the specific type of DNA damage and the resulting response that they induce. For example, while UV-C irradiation can lead to DNA DSBs, the specific role of UV-C in DNA damage depends on the replicative state of treated cells, as those breaks usually arise from the replication of unrepaired UV-induced DNA lesions (52, 53). It was possible that UV-C and the other treatments were not efficient in inducing HSATII RNA. Therefore, we tested the effects of zeocin and etoposide. Etoposide, similarly to doxorubicin, is an anticancer agent that poisons topoisomerase II, stabilizing DNA–protein complexes, which ultimately leads to stalled replication forks (54). Zeocin belongs to the bleomycin/phleomycin family of antibiotics and, as a radiomimetic, has similar effects on DNA as ionizing radiation (55). Both drugs induce DNA DSBs (46, 47), and etoposide has been shown to stimulate the expression and retrotransposition of another repeated element, mouse B2 SINE RNA (56, 57). ARPE-19 cells were exposed to increasing concentrations of zeocin or etoposide; and HSATII, CDKN1A, and DINO RNA expression were monitored. Zeocin caused a rapid, dose-dependent induction of HSATII RNA, reaching a ∼500-fold increase relative to untreated cells, at the maximum dose tested (400 μg/mL) (Fig. 1*B*). Etoposide also elevated HSATII RNA levels, reaching a ∼700-fold increase at the highest dose tested (500 μM) (Fig. 1*C*). CDKN1A and DINO RNA expression mirrored HSATII RNA accumulation, reaching a 6- to 7-fold induction in cells exposed to 400 μg/mL of zeocin (Fig. 1*B*) and ∼25-fold induction in cells treated with 500 μM of etoposide (Fig. 1*C*). No ARPE-19 cell toxicity was detected at any drug concentration after a 24-h treatment (Fig. 1 *B* and *C*).

The kinetics of HSATII, CDKN1A, and DINO RNA expression were monitored by RT-qPCR from 0 to 24 h posttreatment (hpt) with zeocin (200 μg/mL) or etoposide (200 μM). HSATII RNA expression started to increase between 7 and 12 hpt with either zeocin or etoposide, reaching a 300-fold induction at 24 hpt compared to solvent control-treated cells (Fig. 1 *D* and *E*). The dynamics of CDKN1A and DINO RNA expression were accelerated compared to HSATII RNA expression, as both transcripts reached their maximum levels within the first 2 to 4 hpt, suggesting a possible decoupling of DDR/p53-dependent pathways from the mechanism regulating HSATII RNA induction.

Zeocin Treatment Substantially Mimics the Transcriptional Effect of HCMV Infection on HSATII RNA Expression. To compare the induction HSATII RNA by virus vs. DNA-damaging agent, ARPE-19 cells were infected with HCMV (1 $TCID_{50}$/cell) or treated with zeocin (100 μg/mL). The infection used an epithelial cell-grown HCMV strain (TB40/E-GFP-epi) that efficiently infects ARPE-19 cells (58). Mock infection and solvent treatment served as controls. After 24 h, RNA was isolated and analyzed by RNA sequencing (RNA-seq). By analyzing only uniquely mapped HSATII reads, RNA-seq analysis confirmed that zeocin effectively induces HSATII expression in ARPE-19 cells (Fig. 2*A*). Moreover, as in HCMV-infected cells (43), HSATII RNA in zeocin-treated cells is produced preferentially from chromosome 1, 2, 10, and 16. We detected a higher prevalence of HSATII-specific reads from chromosome 1 in cells exposed to zeocin (∼15%) compared to only ∼5% of these reads in samples from HCMV-infected cells (Fig. 2*B*). However, in both HCMV- or zeocin-treated cells, the majority (∼86% or 76%, respectively) of HSATII-specific reads mapped to chromosome 16 (Fig. 2*B*).

Read coverage tracks at the HSATII-rich locus on chromosome 16 were mapped with the Integrative Genomics Viewer (IGV) using STAR aligner (59)-created BAM files (Fig. 2*C*). The data from mock-infected and solvent-treated cells showed very few, if any, reads mapped to this HSATII locus (Fig. 2*C*). The read coverage tracks based on RNA-seq data from HCMV-infected or zeocin-treated ARPE-19 cells display a similar distribution in this HSATII-rich locus spanning ∼17 kb of DNA. Therefore, these data strengthened our view that common mechanisms might be responsible for the induction of HSATII RNA in both HCMV-infected and DNA-damaging drug-treated cells.

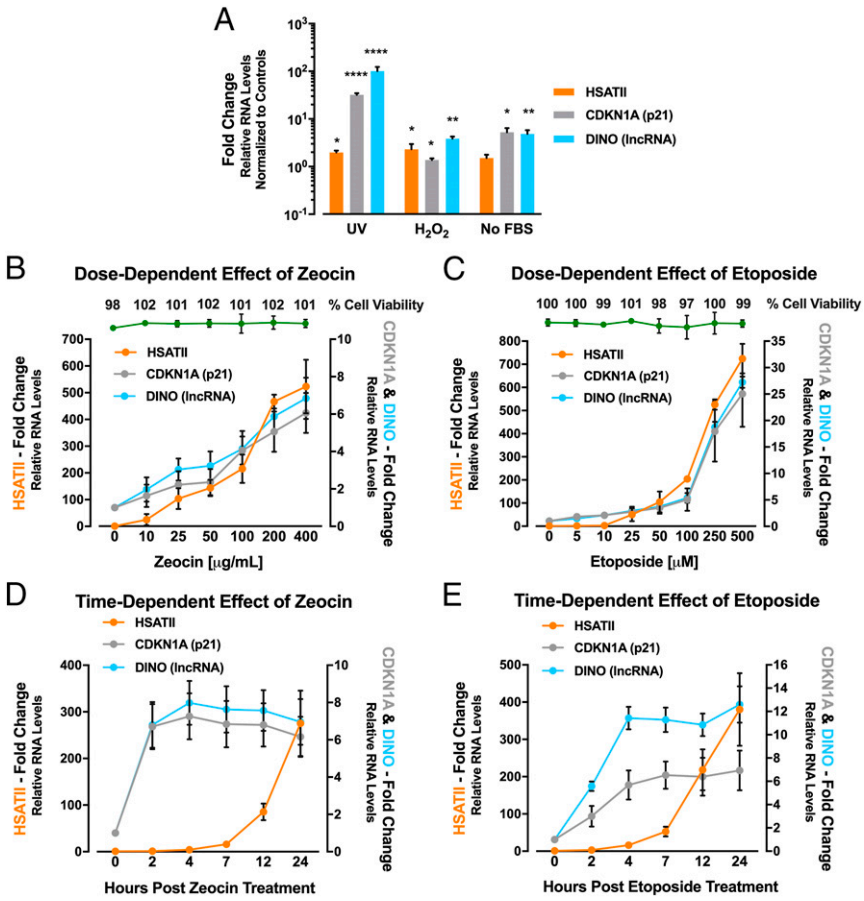

Fig. 1. DDR regulates HSATII RNA expression. (*A*) Limited induction of HSATII RNA by UV, H_2O_2, or serum withdrawal. ARPE-19 cells were exposed to UV irradiation (50 J/m^2), H_2O_2 (100 nM), or serum withdrawal (no FBS). RNA samples were collected at 24 hpt. RT-qPCR was performed to quantify HSATII, CDKN1A, or DINO transcripts, using GAPDH as an internal control. Data are presented as a fold change (mean ± SD; $n = 3$). *$P < 0.05$, **$P < 0.01$, and ***$P < 0.001$. (*B* and *C*) Induction of HSATII RNA by treatment with DNA-damaging drugs. ARPE-19 cells were treated with increasing concentrations of zeocin (*B*) or etoposide (*C*) with H_2O or DMSO, respectively, as solvent controls. RNA samples were collected at 24 hpt, and RT-qPCR was performed to quantify HSATII, CDKN1A, and DINO transcripts, using GAPDH as an internal control. Data are presented as a fold change (mean ± SD; $n = 3$). (*Inset*) At 24 hpt, cell viability was assessed at each indicated drug concentrations. Data are presented as percent viable cells (mean ± SD; $n = 3$). (*D* and *E*) Drug-induced HSATII RNA accumulation occurs after a delay. ARPE-19 cells were treated with zeocin (200 μg/mL) (*D*), etoposide (200 μM) (*E*), and H_2O or DMSO, respectively, as solvent controls. RNA samples were collected at indicated times. RT-qPCR was performed to quantify HSATII, CDKN1A, and DINO transcripts, using GAPDH as an internal control. Data are presented as a fold change (mean ± SD; $n = 3$).

Zeocin Treatment Mimics Aspects of the HCMV-Induced Transcriptome. To assess common biological processes regulated by infection and drug, ARPE-19 cells were HCMV-infected or zeocin-treated (100 μg/mL), and mock infection or solvent treatment served as controls. RNA-seq analysis determined that 654 and 914 cellular RNAs were significantly ($q < 0.05$) modulated in HCMV-infected and zeocin-treated cells, respectively, and 87 RNAs were modulated by both treatments (Fig. 3*A* and *SI Appendix*, Table S1). The 87 coregulated genes were further examined by the gene set enrichment analysis (GSEA) (60) using the hallmark gene set of the Molecular Signatures Database (MSigDB) (61) and found to be strongly associated with multiple gene subsets related to DNA damage/repair and other processes, which, if deregulated, associate with enhanced cancer progression (62–65) (Fig. 3*B*). As we were interested in determining the common molecular mechanisms that govern HSATII RNA induction in infected and zeocin-treated cells, we focused on the role of HCMV- and drug-induced DDR pathways in HSATII RNA expression and its possible effect on cancer cell biology.

ATM Is Required for HSATII RNA Expression. Different types of DNA damage govern the activation of DDR pathways through key regulators: ATM, ATR, and DNA-PKcs (66–68), and each of these PI3-kinases, when activated, phosphorylates the histone H2A family member, H2AX, generating γ-H2AX (69). HCMV infection induces accumulation of γ-H2AX (44, 45) as does zeocin (70). To confirm that both agents induce this marker in ARPE-19 epithelial cells, untreated, HCMV-infected, or zeocin-treated (100 μg/mL) cells were fixed after 24 h, stained with antibody recognizing γ-H2AX protein, and representative images were captured. Both HCMV-infected and zeocin-treated cells had elevated γ-H2AX signals (*SI Appendix*, Fig. S1 *A* and *B*).

We next scrutinized possible contributions of ATM, ATR, and/or DNA-PKcs to HSATII RNA accumulation. ARPE-19 cells were transfected with non-targeting small interfering RNA (NT siRNA) or siRNAs targeting ATM, ATR, or PRKDC (encodes DNA-PKcs) transcripts. Forty-eight hours later, the cells were infected with HCMV or treated with zeocin (100 μg/mL) for 24 h. All specific siRNAs efficiently reduced their targeted transcripts (75 to 90% decrease) (Fig. 4*A*). However, only ATM-specific siRNA treatment led to a significant reduction of HSATII RNA levels (~70% decrease) in HCMV-infected (Fig. 4 *A*, *Left*) or zeocin-treated cells (Fig. 4 *A*, *Right*). To directly assess the importance of ATM kinase activity (68, 71, 72) in HSATII RNA induction, the effect of KU-55933 or AZ31,

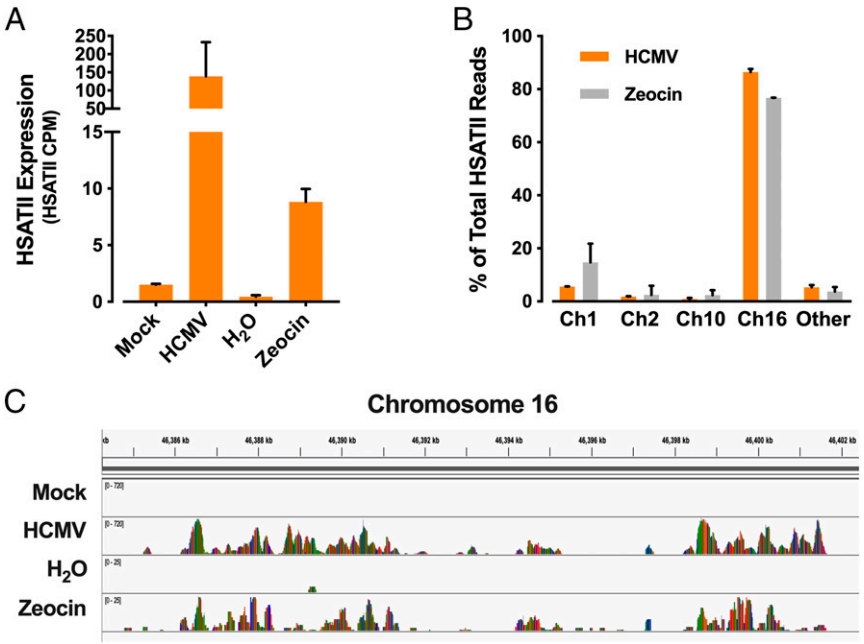

Fig. 2. Zeocin treatment partially mimics the transcriptional effect of HCMV infection on HSATII RNA expression. ARPE-19 cells were infected with HCMV (1 $TCID_{50}$/cell), or treated with zeocin (100 μg/mL) or H_2O as a solvent control, and RNA samples were collected at either 24 hpi or 24 hpt, respectively. RNA was isolated and analyzed using RNA-seq. (*A*) Quantification of HSATII RNA induction by RNA-seq analysis. HSATII RNA expression in terms of counts per million reads mapped (cpm) was computed and normalized across samples ($n = 2$). (*B*) Chromosomal distribution of HSATII RNA expression. HSATII chromosomal origin in HCMV-infected or zeocin-treated cells was depicted based on the number of unique HSATII reads mapped to specific chromosomal loci. Data are presented as a percentage of total HSATII reads (mean ± SD; $n = 2$). (*C*) Example loci of HSATII RNA expression on chromosome 16. HSATII read coverage for HCMV infection vs. zeocin treatment was based on reads mapped to human genome and read coverage track at the HSATII locus on chromosome 16 was visualized using IGV. The nucleotide sequence is represented by colored bars (A - green; C - blue; G - yellow; T - red).

ATM kinase inhibitors (73, 74), were tested. Neither drug compromised the viability of ARPE-19 cells when tested at concentrations up to 50 μM (Fig. 4 *B*, *Left*). However, because we noticed morphological changes in treated cells at the highest dose (50 μM), we used KU-55933 and AZ31 at 20 μM, which is in the range of concentrations at which these drugs are typically used (73–75). Cells were pretreated with KU-55933 or AZ31 for 2 h before being treated with zeocin (100 μg/mL). Interestingly, at 24 hpt, neither ATM kinase inhibitor affected HSATII RNA levels (Fig. 4 *B*, *Right*). However, both kinase inhibitors negatively (~70% decrease) affected expression of CDKN1A and DINO transcripts when compared to DMSO-treated control cells, demonstrating that the drugs were active.

To further establish a role for ATM in HSATII RNA expression, we used ataxia–telangiectasia fibroblasts, A-T(−) cells, that carry a missense mutation in the carboxyl-terminal PI3-kinase-like domain of ATM, and contain very low levels of mutant protein (76, 77). A derivative of this cell line, A-T(+) cells, with a stably expressed, functional ATM gene (77) was used as a control. Cells were HCMV-infected or treated with zeocin (100 μg/mL). Mock infection and solvent treatment served as controls. After 24 h, infected or drug-treated A-T(+) cells were characterized by a 71× or 137× induction of HSATII RNA, respectively; and zeocin-treated, but not HCMV-infected, cells contained higher levels of CDKN1A and DINO RNA. HSATII RNA was also induced in A-T(−) cells following HCMV infection or zeocin treatment, but to a ~6-fold lower level when compared to A-T(+) cells (Fig. 4*C*). Both treatments resulted in significantly lower expression of CDKN1A and DINO RNAs (~15× and ~5× lower, respectively) in A-T(−) cells when compared to A-T(+) cells. Together, these data further implicate ATM in HSATII RNA expression following infection or treatment with DNA-damaging drugs.

Next, to confirm a kinase-independent role for ATM in HSATII RNA expression, we ectopically expressed wild-type ATM (ATM*wt*), kinase-dead ATM (ATM*mut*) or GFP, as a control, in the A-T(−) fibroblasts and followed with zeocin treatment. As demonstrated previously (77), A-T(−) fibroblasts are characterized by a very low level of ATM protein and transfection of the cells with ATM-encoding plasmids resulted in the efficient expression of ATM*wt* or ATM*mut* (Fig. 4 *D*, *Left*). ATM*wt*- but not ATM*mut*-expressing cells responded to zeocin treatment with enhanced phosphorylation of Chk2 at threonine 68, as predicted. HSATII RNA levels were monitored in these cells. Similarly to the data presented in Fig. 4*C*, zeocin treatment increased HSATII expression in untransfected or GFP A-T(−) cells (Fig. 4 *D*, *Right*). Importantly, however, both ATM*wt*- and ATM*mut*-expressing A-T(−) cells responded to zeocin treatment with similarly increased HSATII RNA expression, when compared to untransfected or GFP-expressing cells. Therefore, ATM regulates HSATII expression, but independently from its kinase activity.

HSATII RNA Expression Is Induced by ATM via a Chk1/2- and p53-Independent Pathway. ATM and ATR phosphorylate two downstream kinases, checkpoint 1 and 2 (Chk1 and Chk2 encoded by the CHEK1 and CHEK2 genes, respectively), which ultimately regulate p53 activity in a context-dependent manner (68, 71, 72). Chk2 is normally activated by ATM-mediated phosphorylation, so we tested whether it is required for accumulation of HSATII RNA. As a control, we also tested Chk1. Forty-eight hours prior to HCMV infection or treatment with zeocin (100 μg/mL), ARPE-19 cells were transfected with NT siRNA or siRNA specifically targeting CHEK1 or CHEK2 transcripts. The treatment resulted in a robust decrease in these transcripts at 24 hpi or 24 hpt (Fig. 5*A*). However, we did not

A

B

Gene Set Name	p-value	FDR q-value
HALLMARK_E2F_TARGETS	$2.64\ e^{-17}$	$1.32\ e^{-15}$
HALLMARK_G2M_CHECKPOINT	$3.31\ e^{-11}$	$8.26\ e^{-10}$
HALLMARK_EPITHELIAL_MESENCHYMAL_TRANSITION	$9.52\ e^{-5}$	$1.59\ e^{-3}$
HALLMARK_INTERFERON_GAMMA_RESPONSE	$1.13\ e^{-3}$	$1.13\ e^{-2}$
HALLMARK_MTORC1_SIGNALING	$1.13\ e^{-3}$	$1.13\ e^{-2}$
HALLMARK_HEDGEHOG_SIGNALING	$3.04\ e^{-3}$	$2.53\ e^{-2}$
HALLMARK_DNA_REPAIR	$4.87\ e^{-3}$	$3.48\ e^{-2}$
HALLMARK_APOPTOSIS	$5.92\ e^{-3}$	$3.7\ e^{-2}$

Fig. 3. Zeocin treatment partially mimics the HCMV-induced transcriptome. ARPE-19 cells were mock- or TB40/E-GFP-epi–infected (1 $TCID_{50}$/cell), or treated with zeocin (100 μg/mL) or H_2O as a solvent control. After 24 h, RNA samples were collected and RNA was isolated and analyzed using RNA-seq. (*A*) Cellular genes modulated by both HCMV and zeocin. Venn diagram showing significantly expressed genes either in HCMV-infected or zeocin-treated cells vs. respective controls. (*B*) Categories of gene sets modulated by both HCMV and zeocin. GSEA was performed on the genes differentially expressed in both HCMV-infected and zeocin-treated cells using the hallmark gene set of MSigDB. Identified specific gene set names are categorized based on increasing *P* value and FDR *q* value.

detect a statistically significant decrease of HSATII RNA levels in CHEK1 or CHEK2 KD cells upon HCMV infection or zeocin treatment, consistent with the lack of a requirement for ATM kinase activity (Fig. 4), and further arguing that the canonical ATM-Chk2 signaling cascade does not play an important role in the expression of HSATII RNA.

Since ATM (78) and Chk2 (79) both phosphorylate and stabilize/activate p53, we also investigated the possible involvement of p53 in HSATII RNA induction. Control and p53 KD ARPE-19 cells were HCMV-infected or treated with zeocin (100 μg/mL), and HSATII, CDKN1A, and DINO RNA expression were assessed at 24 (Fig. 5*B*) and 120 hpi/hpt (Fig. 5*C*). TP53-specific siRNA strongly decreased the targeted p53 transcript at both times tested (~83% and 87%), when compared to NT siRNA-treated cells. p53 KD had a modest effect (10% decrease) on HSATII RNA expression at 120 hpi when compared to control cells, but either had no effect (24 hpt) or slightly increased HSATII RNA expression (120 hpt) in zeocin-treated cells. In control experiments, p53 KD had little effect on CDKN1A and DINO expression at 24 h post-HCMV infection, but significantly decreased (~65%) both transcripts at 120 hpi. In comparison, p53 KD strongly (80% decreased) affected CDKN1A and DINO expression at both 24 and 120 h post-zeocin treatment.

In sum, ATM protein is required for HSATII RNA accumulation in response to infection or zeocin treatment. However, ATM kinase activity and two downstream elements of the DDR response that are normally activated by ATM-mediated phosphorylation, Chk2 and p53, are not needed for HSATII RNA expression.

Breast Cancer Cells Differ in HSATII RNA Levels and Sensitivity to HCMV Infection and Zeocin Treatments. HSATII RNA expression has been detected in several cancers, including breast (10, 12), and HSATII copy number gains are a common and negative prognostic feature of colorectal tumors (19). Given the induction of HSATII RNA by HCMV infection (43) and DNA-damaging agents (Fig. 1), and knowing that deregulated DDRs allow cancer cells to achieve high proliferation rates while making them more susceptible to DNA-damaging agents (55, 80), we explored the consequences of induced HSATII RNA expression in breast cancer cells. Initially, we assessed HSATII RNA expression levels in breast cancer cell lines that differed by p53 status, hormonal dependency, and invasiveness (Fig. 6*A*). We tested less invasive tumor cell lines: MDA-MB-175VII (ER+, PR−, HER2-, p53 wt), MDA-MB-361 (ER+, PR+/−, HER2-, p53 wt), MCF7 (ER+, PR+, HER2−, p53 wt); more invasive triple-negative breast cancer (TNBC) cell lines with mutated p53: SUM1315M02, MDA-MB-231, BT-549; and "normal" MCF-10A breast epithelial cells as well as "normal" diploid ARPE-19 cells (81). Cells were cultured in an adherent, two-dimensional format using identical media conditions across all lines to prevent variations in results potentially caused by different culture conditions. Upon reaching 80 to 90% confluency, RNA samples were collected. The basal levels of HSATII RNA in the three less invasive cell lines (MCF-7, MDA-MB-175VII, and MDA-MB-361) were 5- to 6-fold higher when compared to HSATII expression in ARPE-19 cells; and the three more invasive cell lines (SUM1315M02, MDA-MB-231, BT-549) were characterized with 14- to 53-fold higher levels of HSATII RNA compared to less invasive breast cancer cells or ARPE-19 cells. The normal MCF-10A breast epithelial cells had HSATII RNA levels similar to the less invasive group of tumor cells, suggesting that the basal level of HSATII RNA might be influenced by the tissue origin of tested cells.

Next, we tested the induction of HSATII RNA in a selection of the breast cancer cell lines in response to HCMV infection (Fig. 6*B*). At 48 hpi, all tested cells, except BT-549 cells, demonstrated significantly elevated but varied levels of HSATII RNA (from ~5-fold increase in MCF-7 and MDA-MB-231 to ~100-fold increase in MDA-MB-361 and SUM1315M02) compared to its levels in uninfected cells. As we previously established that HCMV IE1 and IE2 proteins collaborate to induce HSATII RNA (43) and knowing that HCMV replication is limited or abortive in cancer cells (58, 82, 83), we monitored expression of UL123 and UL122 viral transcripts, encoding the IE1 and IE2 proteins. UL123 and UL122 RNA expression was detected in the breast cancer cell lines upon HCMV infection (Fig. 6*B*). However, our data did not detect any correlation between levels of HSATII RNA and viral transcripts.

We also tested the effect of zeocin treatment on HSATII RNA induction in these breast cancer cell lines (Fig. 6*C*). At 24 and 96 hpt, all cell lines responded to zeocin with significantly elevated levels of HSATII RNA compared to its levels in solvent control-treated cells. Additionally, a longer exposure (96 h) of cells to the DNA-damaging drug correlated with even higher expression of HSATII RNA. At 96 hpt, HSATII RNA levels increased by as much as 240-fold in the case of MCF-10A cells.

DNA Damage-Induced HSATII RNA Enhances Motility and Proliferation of Breast Cancer Cells. We previously reported that HSATII RNA KD reduced the motility of HCMV-infected ARPE-19 cells (43). Since HCMV infection and zeocin treatment elevated HSATII RNA expression in breast cancer cell lines (Fig. 6 *B* and *C*), we tested whether induced HSATII RNA influences migration of these cells. Infection of breast cancer cells at a high multiplicity with HCMV leads to viral protein expression in only a portion of the cells (58), and this would confound interpretation of the

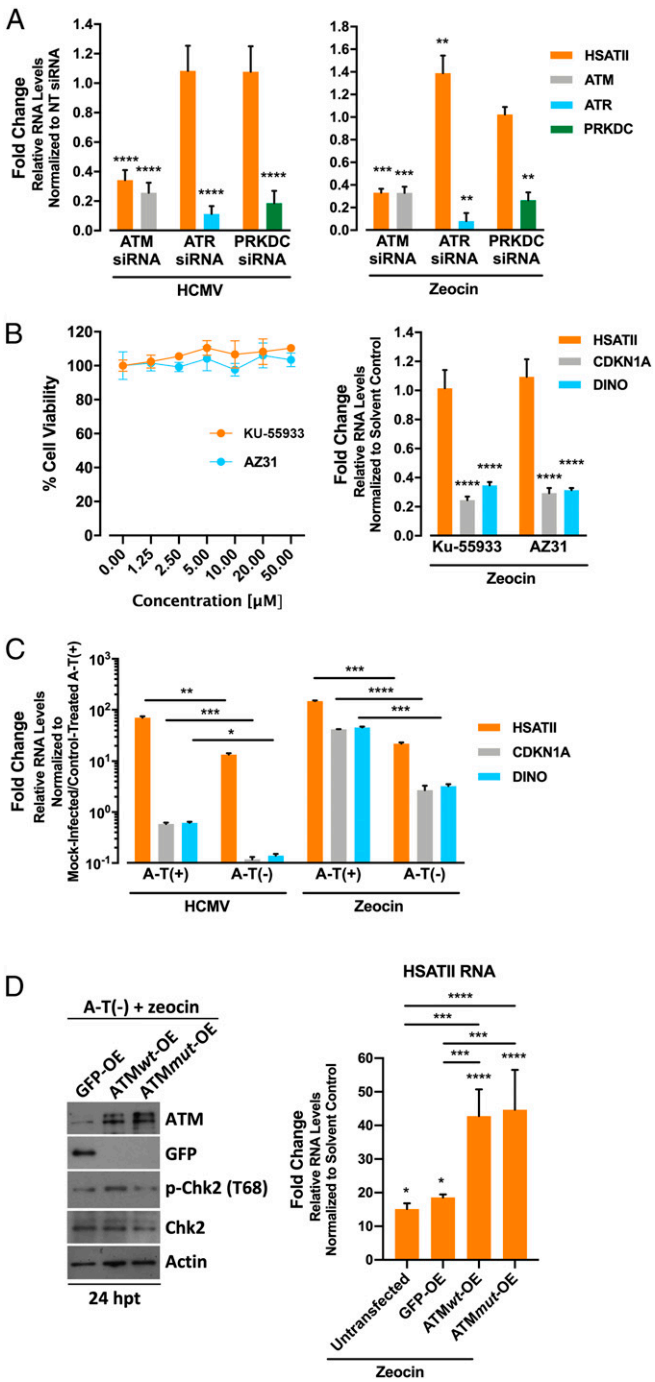

Fig. 4. ATM-based DDR regulates HSATII RNA expression. (*A*) ATM KD inhibits the induction of HSATII RNA by HCMV infection or zeocin treatment. ARPE-19 cells were transfected with ATM-, ATR-, or PRKDC-specific siRNAs or NT siRNA as a control. After 48 h, cells were infected with TB40/E-GFP-epi (1 $TCID_{50}$/cell) or zeocin (100 μg/mL). RNA samples were collected 24 h later. RT-qPCR was performed to quantify HSATII, ATM, ATR, and PRKDC transcripts, using GAPDH as an internal control. Data are presented as a fold change (mean ± SD; $n = 3$–10). (*B*) HSATII RNA is induced less in A-T(−) cells than in A-T(+). A-T(+) and A-T(−) cells were uninfected, infected with TB40/E-GFP (1 $TCID_{50}$/cell), or treated with zeocin (100 μg/mL) or H_2O as a solvent control. RNA samples were collected 24 h later. RT-qPCR was performed to quantify HSATII, CDKN1A, and DINO transcripts, using GAPDH as an internal control. Data are presented as a fold change (mean ± SD; $n = 3$). (*C*) ATM kinase inhibitors do not block the induction of HSATII RNA by zeocin. (*Left*) ARPE-19 cells were treated with various concentrations of KU-55933 or AZ31. At 24 hpt, cell viability was assessed. Data are presented as percent viable cells (mean ± SD; $n = 3$). (*Right*) ARPE-19 cells were treated with DMSO, KU-55933 (20 μM), or AZ31 (20 μM) for 2 h before zeocin (100 μg/mL) was added. RNA samples were collected 24 hpt, and RT-qPCR was performed to quantify HSATII, CDKN1A, and DINO transcripts, and GAPDH was used as an internal control. Data are presented as a fold change (mean ± SD; $n = 3$). (*D*) Ectopic expression of kinase-dead ATM (ATM*mut*) can enhance the induction of HSATII RNA in A-T(−) cells by zeocin. (*Left*) A-T(−) cells were transfected with GFP-, ATM*wt*-, or ATM*mut*-expressing plasmids. After 48 h, cells were exposed to zeocin (100 μg/mL), and protein samples were collected 24 h later. Proteins were assayed by Western blot analysis performed using antibodies recognizing ATM, GFP, phospho-Chk2 (T68), Chk2, and actin as a loading control. (*Right*) A-T(−) cells were transfected with GFP-, ATM*wt*-, or ATM*mut*-expressing plasmids and untransfected cultures served as controls. After 48 h, cells were treated with zeocin (100 μg/mL), and RNA samples were collected 24 h later. RT-qPCR was performed to quantify HSATII. GAPDH was used as an internal control. Data are presented as a fold change (mean ± SD; $n = 4$). $^*P < 0.05$, $^{**}P < 0.01$, $^{***}P < 0.001$, and $^{****}P < 0.0001$.

migration assay. Therefore, we treated ARPE-19, MCF-7, and SUM1315MO2 cells with zeocin (200 μg/mL) or H_2O as a solvent control to guarantee a uniform effect across the cell population (Fig. 7*A*). At 24 hpt, transwell migration assays (84) were performed using equal numbers of cells, and cell motility was assessed after an additional 24 h. ARPE-19 and MCF-7 cells showed an ∼70% and 100% increase in migration, respectively, upon zeocin treatment when compared to solvent control-treated cells. Interestingly, this phenomenon was not observed with SUM1315MO2 cells. Indeed, zeocin caused a slight decrease in the motility of these cells. Although additional cell lines must be assayed to reach a firm conclusion, this result raises the possibility that cells with high basal HSATII RNA levels might be less sensitive to zeocin treatment.

As MDA-MB-231, BT-549, and SUM1315MO2 cells are highly metastatic (85, 86), we tested effects of HSATII RNA KD on the migratory abilities of these three TNBC cells using transwell migration and wound healing (87) assays. For the transwell migration assay, MDA-MB-231, BT-549, and SUM1315MO2 cells were transfected with either non-targeting LNA (NT-LNA) or HSATII-specific LNAs (HSATII-LNAs), and motility was assessed 24 h later (Fig. 7*B*). HSATII-deficient MDA-MB-231, BT-549, and SUM1315 cells exhibited significantly reduced migration relative to control-treated cells. MDA-MB-231 and BT-549 cells were the most sensitive to the treatment with HSATII-LNAs, exhibiting 20- and 5-fold decreases in mean migration, respectively. The wound healing assay provided consistent results (Fig. 7*C*). HSATII-deficient MDA-MB-231, BT-549, and SUM1315 cells were significantly slower in closing wounds compared to control treated cells.

As the aggressiveness of TNBC cells is also related to their high proliferation rates, we tested the effects of HSATII KD on the proliferation of MDA-MB-231, BT-549, and SUM1315MO2 cells (Fig. 7*D*). MDA-MB-231, BT-549, and SUM1315MO2 cells were transfected with either NT-LNA or HSATII-LNAs, and 24 h later equal numbers of cells were seeded in two-dimensional cultures and cell proliferation monitored for 5 consecutive days. Although the cell lines proliferated at different rates, the growth rate was significantly reduced for each cell line following HSATII KD.

Our data suggest that HSATII RNA is an important regulator linking a DDR with processes involved in cancer cell migration and proliferation. Furthermore, at least some DNA-damaging cancer therapeutics, through the induction of HSATII RNA, might enhance the migration and proliferation of tumor cells.

Discussion

Given the ability of HCMV IE1 and 2 proteins to induce a DDR (44, 45) and HSATII RNA (43), and knowing that DNA damage-inducing treatments stimulate the expression of SINEs (56, 57), we tested the possibility that a chemically induced DDR can also induce HSATII RNA. Zeocin and etoposide robustly

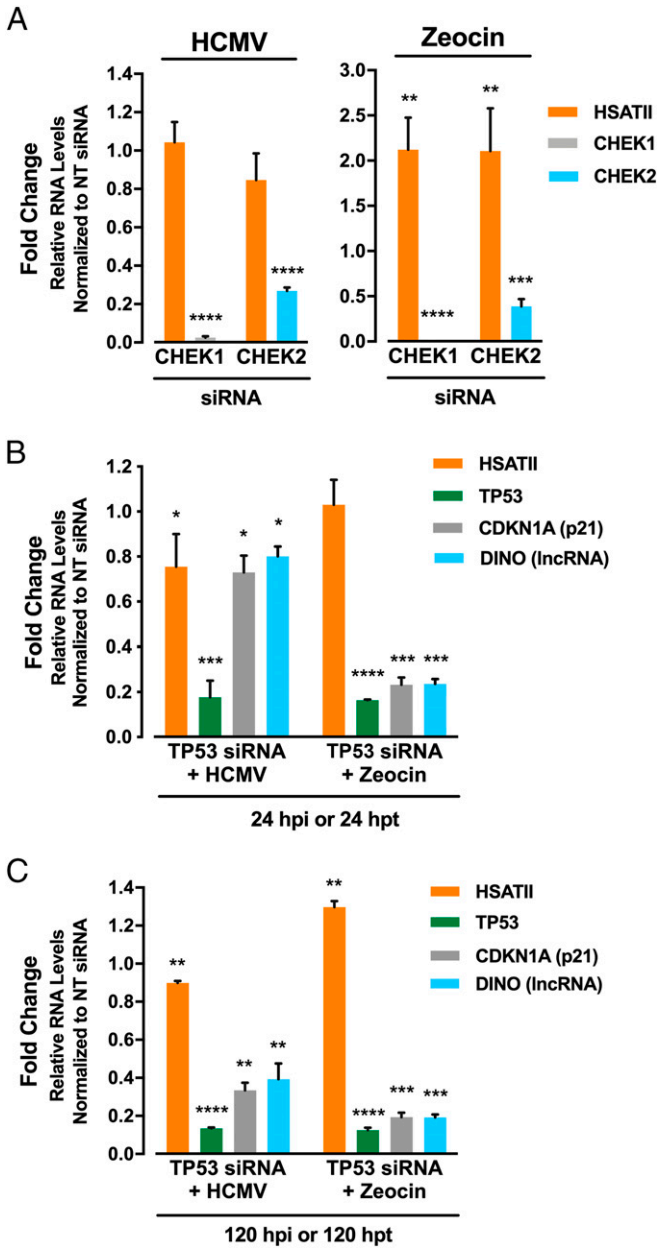

Fig. 5. HSATII RNA expression is induced via a Chk1/2- and p53-independent pathway. (*A*) CHEK1 or CHEK2 KD does not block HSATII RNA induction by infection or zeocin. ARPE-19 cells were transfected with CHEK1- or CHEK2-specific siRNA or NT siRNA as a control. After 48 h, cells were infected with TB40/E-GFP-epi (1 $TCID_{50}$/cell) or zeocin (100 μg/mL). RNA samples were collected 24 h later. RT-qPCR was performed to quantify HSATII, CHEK1, and CHEK2 transcripts, using GAPDH as an internal control. Data are presented as a fold change (mean ± SD; $n = 4$). (*B* and *C*) p53 KD does not block HSATII RNA induction following HCMV infection or zeocin treatment. ARPE-19 cells were transfected with TP53 siRNAs or NT siRNA as a control. After 48 h, cells were infected with TB40/E-GFP-epi (1 TCID/cell) or zeocin (100 μg/mL), and RNA samples were collected 24 h (*B*) or 120 h (*C*) later. RT-qPCR was performed using specific primers to HSATII, TP53, CDKN1A, or DINO transcripts. GAPDH was used as an internal control. Data are presented as a fold change (mean ± SD; $n = 3$–4). $^{*}P < 0.05$, $^{**}P < 0.01$, $^{***}P < 0.001$, and $^{****}P < 0.0001$.

induced HSATII RNA in diploid ARPE-19 epithelial cells (Fig. 1 *B* and *C*) with kinetics (Fig. 1 *D* and *E*) similar to those described previously for the induction of the transcript by HCMV infection (43). In contrast, UV-C did not induce HSATII (Fig. 1*A*). UV-C causes helix-distorting lesions in DNA, such as pyrimidine(6-4)pyrimidone photoproducts and cyclobutane pyrimidine dimers (52), that can subsequently be converted into DSBs during DNA replication; whereas zeocin (88), etoposide (89), and HCMV infection (90) directly induce DSBs. Our UV-C assay employed confluent monolayers of cells, conditions that did not favor cellular DNA replication and induction of DSBs, so it is possible that extensive DNA DSBs were not produced during the course of the experiment.

Zeocin induced expression from a similar set of HSATII loci as did HCMV infection (Fig. 2 *B* and *C*), and a subset of genes induced by zeocin and virus infection overlapped and included key elements of DDR signaling cascades. Infection and zeocin treatment induced γ-H2AX foci in diploid epithelial cells, a marker for DSBs (*SI Appendix*, Fig. S1). The ATM kinase is the primary mediator of the response to DSBs (91), and KD of ATM in diploid epithelial cells (Fig. 4 *A* and *B*) blocked HSATII RNA induction by the DNA-damaging drugs and infection. Zeocin, etoposide, and virus infection each induce a DDR and HSATII RNA, and these responses depend on ATM. However, although ATM protein is required, two different active ATM kinase inhibitors (KU-55933 and AZ31) failed to block HSATII RNA induction by zeocin (Fig. 4*B*). Moreover, ectopic expression of wild-type ATM or kinase-dead ATM restored the ability of ATM-deficient ataxia–telangiectasia A-T(−) cells to efficiently induce HSATII RNA in response to zeocin treatment (Fig. 4*D*). Furthermore, KD of Chk2, which is activated by ATM-mediated phosphorylation, and KD of p53, which is phosphorylated and activated by both ATM and Chk2, had no negative effects on HSATII RNA induction by zeocin (Fig. 5). Thus, our data indicate that ATM kinase activity and the canonical ATM–Chk2–p53 signaling cascade are not required for HSATII RNA accumulation. Different signaling events fit with the observation that the ATM kinase-dependent induction of CDKN1A and DINO RNAs occurs much more rapidly than the ATM kinase-independent induction of HSATII in response to zeocin (Fig. 1*D*) or etoposide (Fig. 1*E*).

Even though its kinase activity is not essential, ATM protein (or mRNA) is clearly required for HSATII RNA induction. There is precedent for ATM kinase-independent function. ATM controls mitophagy through its interaction with the Parkin E3 ubiquitin ligase; ATM acts via the protein–protein interaction, independently of its kinase activity (92). We anticipate that the kinase-independent role of ATM in the induction of HSATII RNA might be driven by a similar mechanism.

Overexpression of HSATII RNA has been reported for lung, ovarian, prostate, and osteosarcoma tumors as well as tumor-derived cell lines (10, 12, 13). Given our current data revealing the importance of the DDR in HSATII RNA expression and with the known impact of deregulated DDRs and cell cycle checkpoints on oncogenesis (93, 94), we probed the physiological consequences of HSATII RNA expression in cultured tumor cells. We tested several breast cancer cell lines growing in adherent, two-dimensional culture, and higher endogenous HSATII RNA levels correlated with a highly metastatic phenotype (Fig. 6*A*), and HSATII levels were substantially increased in most cell lines by HCMV infection or zeocin treatment (Fig. 6 *B* and *C*). Cells characterized by low basal HSATII RNA expression, i.e., ARPE-19 and MCF-7 cells, showed an enhanced migratory phenotype when exposed to zeocin, while SUM1315MO2 cells with higher uninduced levels of HSATII RNA did not (Fig. 7*A*). Perhaps the nonresponsive cells had a sufficiently high level of the satellite RNA before induction. HSATII RNA KD markedly reduced migration (Fig. 7 *B* and *C*) and proliferation (Fig. 7*D*) in the three TNBC cell lines tested, suggesting a direct relationship between high levels of the RNA and cell phenotype. These observations argue that higher HSATII RNA levels

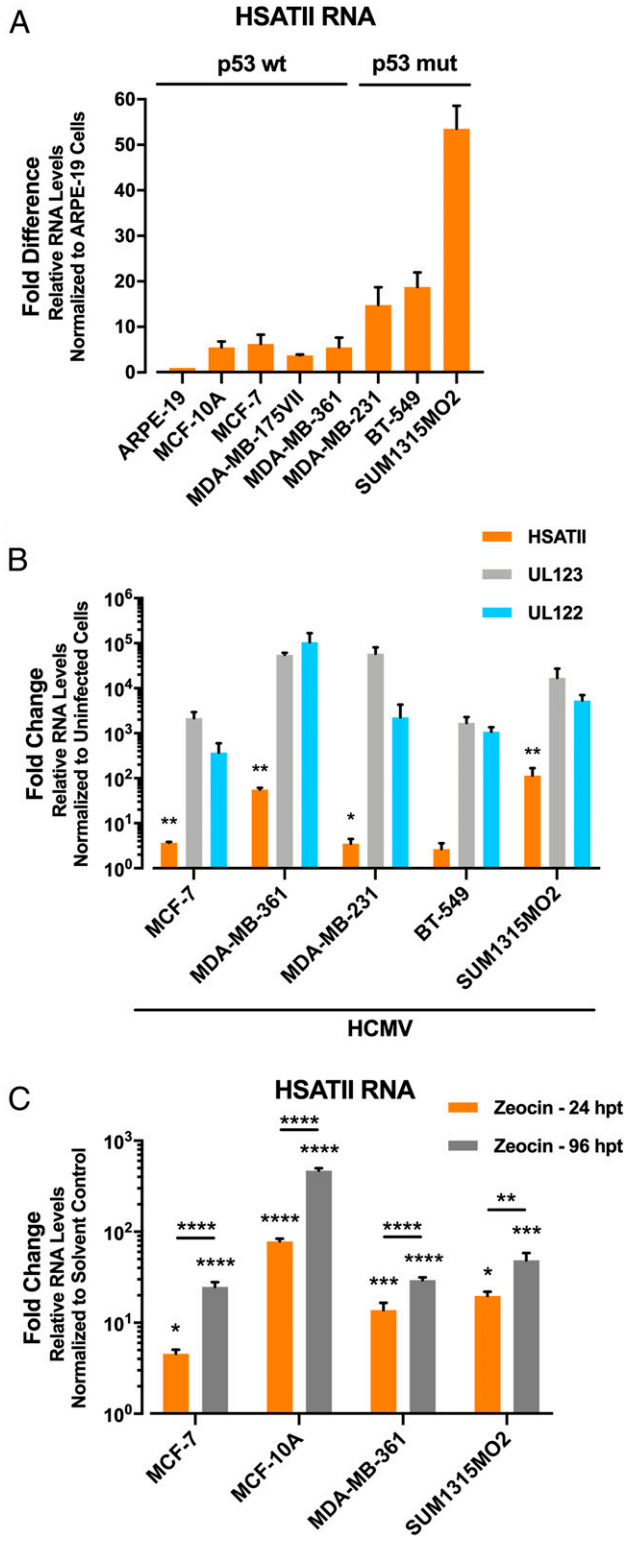

Fig. 6. Breast cancer cells differ in HSATII RNA levels and sensitivity to HCMV infection and zeocin treatment. (*A*) Breast cancer cell lines contain HSATII RNA when grown in adherent (two-dimensional) culture. Cell lines were grown to ~80% confluency and RNA samples were collected. RT-qPCR was performed to quantify HSATII RNA, using GAPDH as an internal control. Data are presented as a fold change (mean ± SD; $n = 3$). (*B*) HCMV infection elevates HSATII RNA levels in breast cancer cell lines. MCF-7, MDA-MB-361, MDA-MB-231, BT-549, and SUM1315MO2 cells were infected with TB40/E-GFP-epi (4 $TCID_{50}$/cell), and RNA samples were collected at 24 hpi. RT-qPCR was performed to quantify HSATII RNA, using GAPDH as an internal control. For UL123 and UL122 RNA, their background Ct values in uninfected cells were used to calculate the fold change expression in infected cells. Data are presented as a fold change (mean ± SD; $n = 3$–5). (*C*) Zeocin treatment elevates HSATII RNA levels in breast cancer cell lines. MCF-7, MCF-10A, MDA-MB-361, and SUM1315MO2 cells were treated with zeocin (200 μg/mL). RNA samples were collected at 24 and 96 hpt, and RT-qPCR was performed to quantify HSATII RNA, using GAPDH as an internal control. Data are presented as a fold change (mean ± SD; $n = 3$). *$P < 0.05$, **$P < 0.01$, ***$P < 0.001$, and ****$P < 0.0001$.

correlate with enhanced proliferation and migration, characteristics of aggressive, metastatic tumors; and they are consistent with an earlier report showing that HSATII copy number gains are a negative prognostic feature of colorectal cancers (19). Of note, numerous noncoding RNAs have been shown to influence tumor cell movement, including miRNAs (95, 96), lncRNAs (97, 98), and circRNAs (99).

DNA-damaging cancer therapeutics can lead to drug resistance (55, 80) and raise concerns about the development of de novo primary tumors (100). The induction of HSATII RNA accumulation by DNA-damaging drugs in cultured cells (Figs. 1 and 6) and the correlation between elevated HSATII RNA and enhanced tumor cell proliferation and migration (Fig. 7) prompt us to speculate that DNA-damaging chemotherapeutics have potential to enhance malignancy of tumor cells that survive treatment. This effect could be of long or short duration, depending on how long HSATII RNA remains elevated after drug treatment. Negative consequences could derive from immediate effects of HSATII RNA overexpression, as we have measured here, and perhaps overexpression of other noncoding RNAs. In addition, longer-term effects might result from reverse transcription of the overexpressed RNAs followed by integration and copy number expansion in tumors, as described for HSATII (19) and another repeated element, LINE-1 (101).

HCMV RNAs and proteins are found in a variety of human malignancies, and HCMV-infected cells have many properties suggesting the virus might influence tumor progression (102), including increased movement (43, 103–106). The ability of HCMV infection, like radiomimetic drugs, to sponsor a DDR (45, 107) with induction of HSATII RNA in healthy cells (43) (Figs. 1 and 2) and breast cancer cells (Fig. 6*B*) leads to a second speculation. Perhaps HSATII RNA induction contributes to the apparent oncomodulatory activity of the virus. Indeed, numerous viruses, many of which are considered tumor viruses, are known to induce a DDR (44); and, therefore, might also induce HSATII RNA contributing to malignancy. For HCMV, even a limited or abortive viral replication documented in cancer cells (58, 82, 83) might lead, via IE1/IE2 protein-mediated HSATII RNA induction, to enhanced migratory and proliferative characteristics of cancer cells.

In sum, this study demonstrates that DNA DSBs induce HSATII RNA via a DDR that requires ATM protein but not its kinase activity, demonstrates a link between expression of the RNA and cellular growth and migration phenotype, and establishes a paradigm to study the biological consequences of HSATII RNA expression—treatment of normal diploid and tumor cells with DNA-damaging agents.

Materials and Methods

Cells, Viruses, and Drugs. Human retinal pigment epithelial (ARPE-19) cells, human foreskin fibroblasts (HFFs) (32), and breast epithelial (MCF-10A) cells, as well as breast cancer cell lines MCF-7, MDA-MB-175VII, MDA-MB-361, and MDA-MB-231 were from the American Type Culture Collection (ATCC). SUM1315MO2 breast cancer cells (108) were generously provided by Stephen Ethier (Medical University of South Carolina). A-T(–) fibroblasts, originally named AT22IJE-T, and A-T(+) fibroblasts with a stably expressed functional ATM were created by the laboratory of Yosef Shiloh (Tel Aviv University School of Medicine, Tel Aviv, Israel) (76, 77) and generously provided by Matthew Weitzman (Perelman School of Medicine, University of

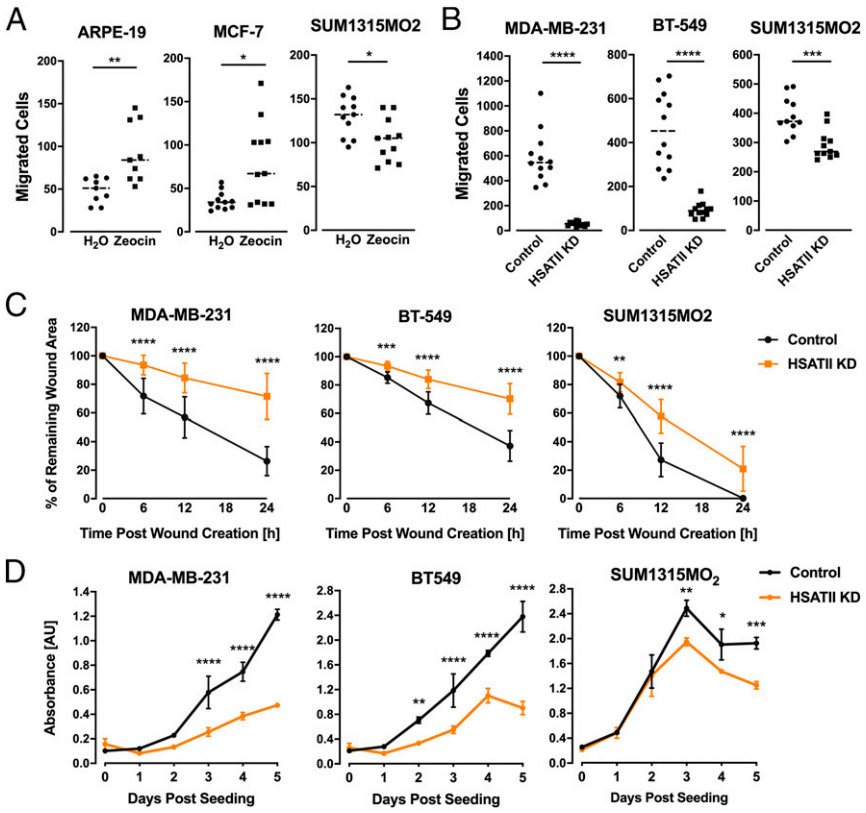

Fig. 7. DNA damage-induced HSATII RNA enhances motility and proliferation of breast cancer cells. (*A*) Zeocin treatment increases migration of cells with low basal levels of HSATII RNA. ARPE-1, MCF-7, and SUM315MO2 cells were treated with zeocin (200 μg/mL) for 24 h. Cells were transferred onto transwell inserts, and 24 h later, migrated cells were washed and fixed, and nuclei were stained. The graph presents a number of cells (with their indicated means) that migrated through a transwell per a field of view (FOV) from biological replicates. $n = 11$. (*B*) Transwell assays demonstrated that HSATII KD reduces migration of breast cancer cells. MDA-MB-231, BT-549, and SUM1315MO2 cells were transfected with NT-LNA or HSATII-LNAs. After 48 hpt, equal number of cells was transferred onto transwell inserts. Twenty-four hours later, migrated cells were washed and fixed, and nuclei were stained. The graph presents a number of cells (with their indicated means) migrated through a transwell per FOV from biological replicates. $n = 12$. (*C*) Wound-healing assays demonstrated that HSATII KD reduces migration of breast cancer cells. MDA-MB-231, BT-549, and SUM1315MO2 cells were transfected with NT-LNA or HSATII-LNAs. After 48 hpt, wounds were created, and their closure was monitored at indicated times. Data from biological replicates are presented as percent of remaining wound width (mean ± SD; $n = 20$). (*D*) HSATII RNA KD reduces the rate of breast cancer cell proliferation in two-dimensional culture. MDA-MB-231, BT-549, and SUM1315MO2 cells were transfected with NT-LNA or HSATII-LNAs. After 48 hpi, equal number of cells was seeded and cell proliferation was monitored at the indicated times. Cell proliferation is presented as an increase in measured absorbance (AU, arbitrary units). $n = 3$. *$P < 0.05$, **$P < 0.01$, ***$P < 0.001$, and ****$P < 0.0001$.

Pennsylvania, Philadelphia, PA). ARPE-19, MCF-7, MDA-MB-175VII, MDA-MB-361, MDA-MB-231, and SUM1315MO2 cells were cultured in 10% FBS/DMEM with added Ham's F-12 nutrient mixture (Sigma-Aldrich) and supplemented with 1× MEM Non-Essential Amino Acids Solution (Thermo Fisher Scientific), 1 mM sodium pyruvate, 1× GlutaMAX, and 10 mM Hepes, pH 7.4. HFFs, A-T(–) cells, and A-T(+) cells were cultured in 10% FBS/DMEM. Media were supplemented with penicillin G sodium salt (100 units/mL) and streptomycin sulfate (95 units/mL).

An infectious BAC clone of HCMV strain TB40/E-GFP (TB40/Ewt-GFP) (109) was electroporated into ARPE-19 cells or HFFs to generate viral progeny that were passaged once more in ARPE-19 cells or HFFs, respectively. TB40/E-GFP-epi designates TB40/E-GFP virus grown in ARPE-19 cells (110). All viral stocks were partially purified by centrifugation through a 20% D-sorbitol cushion in buffer containing 50 mM Tris HCl, 1 mM $MgCl_2$, pH 7.2, resuspended in DMEM and stored in aliquots at −80 °C. Infections were performed by treating cells with viral inoculum for 2 h, followed by removal of the inoculum and washing with PBS (Sigma-Aldrich) before applying fresh medium. Viral stocks were titered by a tissue culture infectious dose 50 ($TCID_{50}$) assay on HFFs or ARPE-19 cells.

Zeocin (InvivoGen) was dissolved in water and stored at −20 °C. Etoposide (Millipore Sigma), KU-55933 (Tocris), and AZ31 (Selleckchem) were dissolved in DMSO and stored at −20 °C.

RNA-Seq Analysis. Total RNA was prepared as described previously (43, 111). Sequencing libraries were prepared using the TruSeq Stranded Total RNA with Ribo-Zero kit (Illumina), and sequenced on Illumina NovaSeq 6000 sequencer instrument in paired-end, rapid mode (2× 150 bp).

For RNA-seq analysis, the Galaxy instance of Princeton University was used (112). RNA-seq data were processed as described previously (43, 111). Human and HCMV fasta and annotation (.gtf) files were created for mapping by combining sequences and annotations from Ensembl annotation, build 38 (GRCh38), Repbase elements (release 19), and TB40 (EF999921) when appropriate. Quality filtered reads were mapped to the concatenated human-virus genomes using RNA STAR (59) (Galaxy, version 2.6.0b-2). The featureCounts program (113) (Galaxy, version 1.6.4) was used to measure gene expression. The resulting files were used as input to determine differential expression for each gene utilizing DESeq2 (114) (Galaxy, version 2.11.40.6). Fold changes in gene expression were considered significant when the adjusted *P* value (*q* value) for multiple testing with the Benjamini–Hochberg procedure, which controls for the false discovery rate (FDR), was <0.05.

To analyze HSATII expression, aligned reads were assigned using the featureCounts function of Rsubread package (115) with the external HSATII annotation obtained from a RepeatMasker (116) using GRCh38 and Repbase consensus sequences. This produced the raw read counts. HSATII expression in terms of cpm (counts per million reads) was computed and normalized across samples using the trimmed mean of M-values method (TMM) (117). To calculate the percent of HSATII reads originating from each chromosome, we identified uniquely mapped reads that exclusively overlapped with HSATII repeat. The number of normalized counts of HSATII reads mapped to each chromosome was computed, and the percentage of these reads mapping to each chromosome was calculated as described previously (43). To visualize read coverage tracks for alignment files, RNA STAR-generated BAM files were imported into the IGV (version 2.6.3) (118) and aligned with

human genome assembly GRCh38 focused on the HSATII locus on chromosome 16. The scale of read coverage peaks was adjusted for experimentally paired samples. To create Venn diagrams, based on data from the DESeq2 analysis the list of significantly expressed genes in HCMV-infected or zeocin-treated cells compared to control cells were imported into a web-based tool InteractiVenn (119).

GSEA (60) was performed on the list of common genes differentially expressed in both HCMV-infected and zeocin-treated cells using the hallmark gene set of the MSigDB (61). A matrix of differentially expressed genes from the dataset significantly matching the hallmark gene set of MSigDB was composed and a list of the hallmark gene subsets was ordered based on a number of overlapping genes, *P* value determining the probability of association with a given gene set, and a FDR *q* value.

Statistical Analysis. Statistical analyses were performed similarly to those described previously (43, 111). To determine statistical significance between two conditions in experiments, unpaired, two-tailed *t* tests with Welch's correction were performed; otherwise, one-way ANOVA was performed between the arrays of data from distinct samples to determine *P* values. A value of $P < 0.05$ was considered significant. Significance is shown by the presence of asterisks above data points with one, two, three, or four asterisks representing $P < 0.05$, $P < 0.01$, $P < 0.001$, or $P < 0.0001$, respectively. Only significant *P* values are reported.

Additional detailed methods are provided in *SI Appendix, SI Materials and Methods*. These describe RNA and protein analysis; immunofluorescence analysis; plasmid transfection; cell stress induction; LNA and siRNA KD procedures; and cell migration, proliferation, and toxicity assays.

Data Availability. Raw RNA-seq data have been deposited in the National Center for Biotechnology Information Gene Expression Omnibus (GEO) database (accession no. GSE159235).

ACKNOWLEDGMENTS. We thank Stephen Ethier (Medical University of South Carolina) for generously providing SUM1315MO2 cells; Matthew Weitzman (Perelman School of Medicine, University of Pennsylvania) for generously providing A-T(–) and A-T(+) fibroblasts, Alexander Solovyov (Memorial Sloan Kettering Cancer Center) for advice and assistance with RNA-seq analyses, and members of the T.S. laboratory for scientific discussions. This work was supported by NIH Grants AI112951 and AI142520. M.T.N. was partially supported by American Cancer Society Fellowship PF-14-116-01-MPC.

1. A. J. Levine, D. T. Ting, B. D. Greenbaum, P53 and the defenses against genome instability caused by transposons and repetitive elements. *BioEssays* **38**, 508–513 (2016).
2. Z. Pezer, J. Brajković, I. Feliciello, D. Ugarković, Satellite DNA-mediated effects on genome regulation. *Genome Dyn.* **7**, 153–169 (2012).
3. A. Eymery *et al*., A transcriptomic analysis of human centromeric and pericentric sequences in normal and tumor cells. *Nucleic Acids Res.* **37**, 6340–6354 (2009).
4. L. E. Hall, S. E. Mitchell, R. J. O'Neill, Pericentric and centromeric transcription: A perfect balance required. *Chromosome Res.* **20**, 535–546 (2012).
5. M. A. Garrido-Ramos, Satellite DNA: An evolving topic. *Genes (Basel)* **8**, 230 (2017).
6. S. Louzada *et al*., Decoding the role of satellite DNA in genome architecture and plasticity-an evolutionary and clinical affair. *Genes (Basel)* **11**, 72 (2020).
7. K. Grønbaek, C. Hother, P. A. Jones, Epigenetic changes in cancer. *APMIS* **115**, 1039–1059 (2007).
8. R. Kanwal, S. Gupta, Epigenetic modifications in cancer. *Clin. Genet.* **81**, 303–311 (2012).
9. A. Sanchez Calle, Y. Kawamura, Y. Yamamoto, F. Takeshita, T. Ochiya, Emerging roles of long non-coding RNA in cancer. *Cancer Sci.* **109**, 2093–2100 (2018).
10. D. T. Ting *et al*., Aberrant overexpression of satellite repeats in pancreatic and other epithelial cancers. *Science* **331**, 593–596 (2011).
11. K. I. Leonova *et al*., p53 cooperates with DNA methylation and a suicidal interferon response to maintain epigenetic silencing of repeats and noncoding RNAs. *Proc. Natl. Acad. Sci. U.S.A.* **110**, E89–E98 (2013).
12. L. L. Hall *et al*., Demethylated HSATII DNA and HSATII RNA foci sequester PRC1 and MeCP2 into cancer-specific nuclear bodies. *Cell Rep.* **18**, 2943–2956 (2017).
13. X. D. Ho *et al*., Analysis of the expression of repetitive DNA elements in osteosarcoma. *Front. Genet.* **8**, 193 (2017).
14. Q. Zhu *et al*., BRCA1 tumour suppression occurs via heterochromatin-mediated silencing. *Nature* **477**, 179–184 (2011).
15. Q. Zhu *et al*., Heterochromatin-encoded satellite RNAs induce breast cancer. *Mol. Cell* **70**, 842–853.e7 (2018).
16. R. Valgardsdottir *et al*., Transcription of Satellite III non-coding RNAs is a general stress response in human cells. *Nucleic Acids Res.* **36**, 423–434 (2008).
17. H. Bouzinba-Segard, A. Guais, C. Francastel, Accumulation of small murine minor satellite transcripts leads to impaired centromeric architecture and function. *Proc. Natl. Acad. Sci. U.S.A.* **103**, 8709–8714 (2006).
18. M. De Cecco *et al*., Genomes of replicatively senescent cells undergo global epigenetic changes leading to gene silencing and activation of transposable elements. *Aging Cell* **12**, 247–256 (2013).
19. F. Bersani *et al*., Pericentromeric satellite repeat expansions through RNA-derived DNA intermediates in cancer. *Proc. Natl. Acad. Sci. U.S.A.* **112**, 15148–15153 (2015).
20. A. Tanne *et al*., Distinguishing the immunostimulatory properties of noncoding RNAs expressed in cancer cells. *Proc. Natl. Acad. Sci. U.S.A.* **112**, 15154–15159 (2015).
21. N. A. Krump, J. You, Molecular mechanisms of viral oncogenesis in humans. *Nat. Rev. Microbiol.* **16**, 684–698 (2018).
22. E. A. Mesri, M. A. Feitelson, K. Munger, Human viral oncogenesis: A cancer hallmarks analysis. *Cell Host Microbe* **15**, 266–282 (2014).
23. M. E. McLaughlin-Drubin, K. Munger, Viruses associated with human cancer. *Biochim. Biophys. Acta* **1782**, 127–150 (2008).
24. M. K. White, J. S. Pagano, K. Khalili, Viruses and human cancers: A long road of discovery of molecular paradigms. *Clin. Microbiol. Rev.* **27**, 463–481 (2014).
25. I. G. Sia, R. Patel, New strategies for prevention and therapy of cytomegalovirus infection and disease in solid-organ transplant recipients. *Clin. Microbiol. Rev.* **13**, 83–121 (2000).
26. S. S. Kanj, A. I. Sharara, P. A. Clavien, J. D. Hamilton, Cytomegalovirus infection following liver transplantation: Review of the literature. *Clin. Infect. Dis.* **22**, 537–549 (1996).
27. G. Gerna *et al*., Human cytomegalovirus end-organ disease is associated with high or low systemic viral load in preemptively treated solid-organ transplant recipients. *New Microbiol.* **35**, 279–287 (2012).
28. T. M. Lanzieri, S. C. Dollard, S. R. Bialek, S. D. Grosse, Systematic review of the birth prevalence of congenital cytomegalovirus infection in developing countries. *Int. J. Infect. Dis.* **22**, 44–48 (2014).
29. M. Michaelis, H. W. Doerr, J. Cinatl, The story of human cytomegalovirus and cancer: Increasing evidence and open questions. *Neoplasia* **11**, 1–9 (2009).
30. G. Herbein, The human cytomegalovirus, from oncomodulation to oncogenesis. *Viruses* **10**, 408 (2018).
31. Q. Lepiller, K. Aziz Khan, V. Di Martino, G. Herbein, Cytomegalovirus and tumors: Two players for one goal-immune escape. *Open Virol. J.* **5**, 60–69 (2011).
32. L. Vastag, E. Koyuncu, S. L. Grady, T. E. Shenk, J. D. Rabinowitz, Divergent effects of human cytomegalovirus and herpes simplex virus-1 on cellular metabolism. *PLoS Pathog.* **7**, e1002124 (2011).
33. P. Kumari *et al*., Essential role of HCMV deubiquitinase in promoting oncogenesis by targeting anti-viral innate immune signaling pathways. *Cell Death Dis.* **8**, e3078 (2017).
34. D. Collins-McMillen *et al*., Human cytomegalovirus promotes survival of infected monocytes via a distinct temporal regulation of cellular bcl-2 family proteins. *J. Virol.* **90**, 2356–2371 (2015).
35. L. Soroceanu, C. S. Cobbs, Is HCMV a tumor promoter? *Virus Res.* **157**, 193–203 (2011).
36. B. Bhattacharjee, N. Renzette, T. F. Kowalik, Genetic analysis of cytomegalovirus in malignant gliomas. *J. Virol.* **86**, 6815–6824 (2012).
37. M. El-Shinawi *et al*., Human cytomegalovirus infection enhances NF-κB/p65 signaling in inflammatory breast cancer patients. *PLoS One* **8**, e55755 (2013).
38. M. Michaelis *et al*., Selection of a highly invasive neuroblastoma cell population through long-term human cytomegalovirus infection. *Oncogenesis* **1**, e10 (2012).
39. P. Ranganathan, P. A. Clark, J. S. Kuo, M. S. Salamat, R. F. Kalejta, Significant association of multiple human cytomegalovirus genomic Loci with glioblastoma multiforme samples. *J. Virol.* **86**, 854–864 (2012).
40. L. Harkins *et al*., Specific localisation of human cytomegalovirus nucleic acids and proteins in human colorectal cancer. *Lancet* **360**, 1557–1563 (2002).
41. L. E. Harkins *et al*., Detection of human cytomegalovirus in normal and neoplastic breast epithelium. *Herpesviridae* **1**, 8 (2010).
42. J. Cinatl, M. Scholz, R. Kotchetkov, J. U. Vogel, H. W. Doerr, Molecular mechanisms of the modulatory effects of HCMV infection in tumor cell biology. *Trends Mol. Med.* **10**, 19–23 (2004).
43. M. T. Nogalski *et al*., A tumor-specific endogenous repetitive element is induced by herpesviruses. *Nat. Commun.* **10**, 90 (2019).
44. E. Xiaofei, T. F. Kowalik, The DNA damage response induced by infection with human cytomegalovirus and other viruses. *Viruses* **6**, 2155–2185 (2014).
45. E. Xiaofei *et al*., An E2F1-mediated DNA damage response contributes to the replication of human cytomegalovirus. *PLoS Pathog.* **7**, e1001342 (2011).
46. D. J. Smart *et al*., Assessment of DNA double-strand breaks and gammaH2AX induced by the topoisomerase II poisons etoposide and mitoxantrone. *Mutat. Res.* **641**, 43–47 (2008).
47. K. Shimada *et al*., TORC2 signaling pathway guarantees genome stability in the face of DNA strand breaks. *Mol. Cell* **51**, 829–839 (2013).
48. T. Waldman, K. W. Kinzler, B. Vogelstein, p21 is necessary for the p53-mediated G1 arrest in human cancer cells. *Cancer Res.* **55**, 5187–5190 (1995).
49. M. Valverde *et al*., Hydrogen peroxide-induced DNA damage and repair through the differentiation of human adipose-derived mesenchymal stem cells. *Stem Cells Int.* **2018**, 1615497 (2018).
50. B. Benedict *et al*., Loss of p53 suppresses replication-stress-induced DNA breakage in G1/S checkpoint deficient cells. *eLife* **7**, e37868 (2018).

51. A. M. Schmitt *et al*., An inducible long noncoding RNA amplifies DNA damage signaling. *Nat. Genet.* **48**, 1370–1376 (2016).
52. L. F. Batista, B. Kaina, R. Meneghini, C. F. Menck, How DNA lesions are turned into powerful killing structures: Insights from UV-induced apoptosis. *Mutat. Res.* **681**, 197–208 (2009).
53. W. P. Roos, B. Kaina, DNA damage-induced cell death: From specific DNA lesions to the DNA damage response and apoptosis. *Cancer Lett.* **332**, 237–248 (2013).
54. S. Liu *et al*., Distinct roles for DNA-PK, ATM and ATR in RPA phosphorylation and checkpoint activation in response to replication stress. *Nucleic Acids Res.* **40**, 10780–10794 (2012).
55. D. Woods, J. J. Turchi, Chemotherapy induced DNA damage response: Convergence of drugs and pathways. *Cancer Biol. Ther.* **14**, 379–389 (2013).
56. C. R. Hagan, R. F. Sheffield, C. M. Rudin, Human Alu element retrotransposition induced by genotoxic stress. *Nat. Genet.* **35**, 219–220 (2003).
57. C. M. Rudin, C. B. Thompson, Transcriptional activation of short interspersed elements by DNA-damaging agents. *Genes Chromosomes Cancer* **30**, 64–71 (2001).
58. A. Oberstein, T. Shenk, Cellular responses to human cytomegalovirus infection: Induction of a mesenchymal-to-epithelial transition (MET) phenotype. *Proc. Natl. Acad. Sci. U.S.A.* **114**, E8244–E8253 (2017).
59. A. Dobin *et al*., STAR: Ultrafast universal RNA-seq aligner. *Bioinformatics* **29**, 15–21 (2013).
60. A. Subramanian *et al*., Gene set enrichment analysis: A knowledge-based approach for interpreting genome-wide expression profiles. *Proc. Natl. Acad. Sci. U.S.A.* **102**, 15545–15550 (2005).
61. A. Liberzon *et al*., The Molecular Signatures Database (MSigDB) hallmark gene set collection. *Cell Syst.* **1**, 417–425 (2015).
62. J. M. Ford, M. B. Kastan, "DNA damage response pathways and cancer" in *Abeloff's Clinical Oncology*, J. E. Niederhuber, J. O. Armitage, M. B. Kastan, J. H. Doroshow, J. E. Tepper, Eds. (Elsevier, Philadelphia, ed. 6, 2020), pp. 154–164.
63. W. Lu, Y. Kang, Epithelial-mesenchymal plasticity in cancer progression and metastasis. *Dev. Cell* **49**, 361–374 (2019).
64. L. C. Kim, R. S. Cook, J. Chen, mTORC1 and mTORC2 in cancer and the tumor microenvironment. *Oncogene* **36**, 2191–2201 (2017).
65. A. Hanna, L. A. Shevde, Hedgehog signaling: Modulation of cancer properies and tumor mircroenvironment. *Mol. Cancer* **15**, 24 (2016).
66. J. Falck, J. Coates, S. P. Jackson, Conserved modes of recruitment of ATM, ATR and DNA-PKcs to sites of DNA damage. *Nature* **434**, 605–611 (2005).
67. G. Giglia-Mari, A. Zotter, W. Vermeulen, DNA damage response. *Cold Spring Harb. Perspect. Biol.* **3**, a000745 (2011).
68. A. N. Blackford, S. P. Jackson, ATM, ATR, and DNA-PK: The trinity at the heart of the DNA damage response. *Mol. Cell* **66**, 801–817 (2017).
69. J. Yuan, R. Adamski, J. Chen, Focus on histone variant H2AX: To be or not to be. *FEBS Lett.* **584**, 3717–3724 (2010).
70. F. Delacôte *et al*., Chronic exposure to sublethal doses of radiation mimetic Zeocin selects for clones deficient in homologous recombination. *Mutat. Res.* **615**, 125–133 (2007).
71. J. Smith, L. M. Tho, N. Xu, D. A. Gillespie, The ATM-Chk2 and ATR-Chk1 pathways in DNA damage signaling and cancer. *Adv. Cancer Res.* **108**, 73–112 (2010).
72. Y. H. Ou, P. H. Chung, T. P. Sun, S. Y. Shieh, p53 C-terminal phosphorylation by CHK1 and CHK2 participates in the regulation of DNA-damage-induced C-terminal acetylation. *Mol. Biol. Cell* **16**, 1684–1695 (2005).
73. I. Hickson *et al*., Identification and characterization of a novel and specific inhibitor of the ataxia-telangiectasia mutated kinase ATM. *Cancer Res.* **64**, 9152–9159 (2004).
74. J. Greene *et al*., The novel ATM inhibitor (AZ31) enhances antitumor activity in patient derived xenografts that are resistant to irinotecan monotherapy. *Oncotarget* **8**, 110904–110913 (2017).
75. Y. Li, D. Q. Yang, The ATM inhibitor KU-55933 suppresses cell proliferation and induces apoptosis by blocking Akt in cancer cells with overactivated Akt. *Mol. Cancer Ther.* **9**, 113–125 (2010).
76. Y. Ziv *et al*., Cellular and molecular characteristics of an immortalized ataxia-telangiectasia (group AB) cell line. *Cancer Res.* **49**, 2495–2501 (1989).
77. Y. Ziv *et al*., Recombinant ATM protein complements the cellular A-T phenotype. *Oncogene* **15**, 159–167 (1997).
78. C. E. Canman *et al*., Activation of the ATM kinase by ionizing radiation and phosphorylation of p53. *Science* **281**, 1677–1679 (1998).
79. A. Hirao *et al*., DNA damage-induced activation of p53 by the checkpoint kinase Chk2. *Science* **287**, 1824–1827 (2000).
80. K. Cheung-Ong, G. Giaever, C. Nislow, DNA-damaging agents in cancer chemotherapy: Serendipity and chemical biology. *Chem. Biol.* **20**, 648–659 (2013).
81. X. Dai, H. Cheng, Z. Bai, J. Li, Breast cancer cell line classification and its relevance with breast tumor subtyping. *J. Cancer* **8**, 3131–3141 (2017).
82. S. Xu, X. Schafer, J. Munger, Expression of oncogenic alleles induces multiple blocks to human cytomegalovirus infection. *J. Virol.* **90**, 4346–4356 (2016).
83. Q. Lepiller, W. Abbas, A. Kumar, M. K. Tripathy, G. Herbein, HCMV activates the IL-6-JAK-STAT3 axis in HepG2 cells and primary human hepatocytes. *PLoS One* **8**, e59591 (2013).
84. C. R. Justus, N. Leffler, M. Ruiz-Echevarria, L. V. Yang, In vitro cell migration and invasion assays. *J. Vis. Exp.* **88**, 51046 (2014).
85. Y. L. Liu *et al*., Assessing metastatic potential of breast cancer cells based on EGFR dynamics. *Sci. Rep.* **9**, 3395 (2019).
86. A. V. Taubenberger, V. M. Quent, L. Thibaudeau, J. A. Clements, D. W. Hutmacher, Delineating breast cancer cell interactions with engineered bone microenvironments. *J. Bone Miner. Res.* **28**, 1399–1411 (2013).
87. C. C. Liang, A. Y. Park, J. L. Guan, In vitro scratch assay: A convenient and inexpensive method for analysis of cell migration in vitro. *Nat. Protoc.* **2**, 329–333 (2007).
88. G. M. Ehrenfeld *et al*., Copper-dependent cleavage of DNA by bleomycin. *Biochemistry* **26**, 931–942 (1987).
89. Y. Pommier, E. Leo, H. Zhang, C. Marchand, DNA topoisomerases and their poisoning by anticancer and antibacterial drugs. *Chem. Biol.* **17**, 421–433 (2010).
90. M. T. Pickering, T. F. Kowalik, Rb inactivation leads to E2F1-mediated DNA double-strand break accumulation. *Oncogene* **25**, 746–755 (2006).
91. C. J. Bakkenist, M. B. Kastan, DNA damage activates ATM through intermolecular autophosphorylation and dimer dissociation. *Nature* **421**, 499–506 (2003).
92. A. Sarkar *et al*., Ataxia telangiectasia mutated interacts with Parkin and induces mitophagy independent of kinase activity. Evidence from mantle cell lymphoma. *Haematologica*, 10.3324/haematol.2019.234385 (2020).
93. P. Bouwman, J. Jonkers, The effects of deregulated DNA damage signalling on cancer chemotherapy response and resistance. *Nat. Rev. Cancer* **12**, 587–598 (2012).
94. F. G. Giancotti, Deregulation of cell signaling in cancer. *FEBS Lett.* **588**, 2558–2570 (2014).
95. B. J. Petri, C. M. Klinge, Regulation of breast cancer metastasis signaling by miRNAs. *Cancer Metastasis Rev.* **39**, 837–886 (2020).
96. R. K. Kanchan, J. A. Siddiqui, S. Mahapatra, S. K. Batra, M. W. Nasser, microRNAs orchestrate pathophysiology of breast cancer brain metastasis: Advances in therapy. *Mol. Cancer* **19**, 29 (2020).
97. L. Liu, Y. Zhang, J. Lu, The roles of long noncoding RNAs in breast cancer metastasis. *Cell Death Dis.* **11**, 749 (2020).
98. X. Chen *et al*., The emerging role of long non-coding RNAs in the metastasis of hepatocellular carcinoma. *Biomolecules* **10**, 66 (2019).
99. Y. Shao, B. Lu, The crosstalk between circular RNAs and the tumor microenvironment in cancer metastasis. *Cancer Cell Int.* **20**, 448 (2020).
100. L. Livraghi, J. E. Garber, PARP inhibitors in the management of breast cancer: Current data and future prospects. *BMC Med.* **13**, 188 (2015).
101. B. Rodriguez-Martin *et al*.; PCAWG Structural Variation Working Group; PCAWG Consortium, Pan-cancer analysis of whole genomes identifies driver rearrangements promoted by LINE-1 retrotransposition. *Nat. Genet.* **52**, 306–319 (2020).
102. C. Cobbs, Cytomegalovirus is a tumor-associated virus: Armed and dangerous. *Curr. Opin. Virol.* **39**, 49–59 (2019).
103. M. S. Smith, G. L. Bentz, J. S. Alexander, A. D. Yurochko, Human cytomegalovirus induces monocyte differentiation and migration as a strategy for dissemination and persistence. *J. Virol.* **78**, 4444–4453 (2004).
104. G. L. Bentz, A. D. Yurochko, Human CMV infection of endothelial cells induces an angiogenic response through viral binding to EGF receptor and beta1 and beta3 integrins. *Proc. Natl. Acad. Sci. U.S.A.* **105**, 5531–5536 (2008).
105. J. Vomaske *et al*., Differential ligand binding to a human cytomegalovirus chemokine receptor determines cell type-specific motility. *PLoS Pathog.* **5**, e1000304 (2009).
106. M. T. Nogalski, G. Chan, E. V. Stevenson, S. Gray, A. D. Yurochko, HCMV-regulated paxillin in monocytes links cellular pathogenic motility to the process of viral entry. *J. Virol.* **85**, 1360–1369 (2011).
107. M. H. Luo, K. Rosenke, K. Czornak, E. A. Fortunato, Human cytomegalovirus disrupts both ataxia telangiectasia mutated protein (ATM)- and ATM-Rad3-related kinase-mediated DNA damage responses during lytic infection. *J. Virol.* **81**, 1934–1950 (2007).
108. R. M. Neve *et al*., A collection of breast cancer cell lines for the study of functionally distinct cancer subtypes. *Cancer Cell* **10**, 515–527 (2006).
109. E. Murphy *et al*., Coding potential of laboratory and clinical strains of human cytomegalovirus. *Proc. Natl. Acad. Sci. U.S.A.* **100**, 14976–14981 (2003).
110. K. Wu, A. Oberstein, W. Wang, T. Shenk, Role of PDGF receptor-α during human cytomegalovirus entry into fibroblasts. *Proc. Natl. Acad. Sci. U.S.A.* **115**, E9889–E9898 (2018).
111. S. Chen, T. Shenk, M. T. Nogalski, P2Y2 purinergic receptor modulates virus yield, calcium homeostasis, and cell motility in human cytomegalovirus-infected cells. *Proc. Natl. Acad. Sci. U.S.A.* **116**, 18971–18982 (2019).
112. E. Afgan *et al*., The Galaxy platform for accessible, reproducible and collaborative biomedical analyses: 2018 update. *Nucleic Acids Res.* **46**, W537–W544 (2018).
113. Y. Liao, G. K. Smyth, W. Shi, featureCounts: An efficient general purpose program for assigning sequence reads to genomic features. *Bioinformatics* **30**, 923–930 (2014).
114. M. I. Love, W. Huber, S. Anders, Moderated estimation of fold change and dispersion for RNA-seq data with DESeq2. *Genome Biol.* **15**, 550 (2014).
115. Y. Liao, G. K. Smyth, W. Shi, The subread aligner: Fast, accurate and scalable read mapping by seed-and-vote. *Nucleic Acids Res.* **41**, e108 (2013).
116. A. F. A. Smit, R. Hubley, P. Green, RepeatMasker Open-4.0 (2013–2015). http://www.repeatmasker.org/. Accessed 23 November 2020.
117. M. D. Robinson, A. Oshlack, A scaling normalization method for differential expression analysis of RNA-seq data. *Genome Biol.* **11**, R25 (2010).
118. H. Thorvaldsdóttir, J. T. Robinson, J. P. Mesirov, Integrative genomics viewer (IGV): High-performance genomics data visualization and exploration. *Brief. Bioinform.* **14**, 178–192 (2013).
119. H. Heberle, G. V. Meirelles, F. R. da Silva, G. P. Telles, R. Minghim, InteractiVenn: A web-based tool for the analysis of sets through Venn diagrams. *BMC Bioinformatics* **16**, 169 (2015).